ResearchGate

See discussions, stats, and author profiles for this publication at: https://www.researchgate.net/publication/263586320

Very Large Cooperative Effects in Heterobimetallic Titanium–Chromium Catalysts for Ethylene Polymerization/Copolymerization

ARTICLE *in* JOURNAL OF THE AMERICAN CHEMICAL SOCIETY · JULY 2014

Impact Factor: 12.11 · DOI: 10.1021/ja5046742 · Source: PubMed

CITATIONS
13

READS
11

5 AUTHORS, INCLUDING:

Alessandro Motta
Consorzio Interuniversitario Nazionale per la …
49 PUBLICATIONS **901** CITATIONS
SEE PROFILE

Aidan R Mouat
Northwestern University
5 PUBLICATIONS **14** CITATIONS
SEE PROFILE

Massimiliano Delferro
Northwestern University
35 PUBLICATIONS **511** CITATIONS
SEE PROFILE

Available from: Massimiliano Delferro
Retrieved on: 24 January 2016

JACS
JOURNAL OF THE AMERICAN CHEMICAL SOCIETY
Article
pubs.acs.org/JACS

Very Large Cooperative Effects in Heterobimetallic Titanium-Chromium Catalysts for Ethylene Polymerization/Copolymerization

Shaofeng Liu,[†] Alessandro Motta,[‡] Aidan R. Mouat,[†] Massimiliano Delferro,*[,†] and Tobin J. Marks*[,†]

[†]Department of Chemistry, Northwestern University, Evanston, Illinois 60208-3113, United States
[‡]Dipartimento di Scienze Chimiche, Università di Catania and INSTM, UdR Catania, 95125 Catania, Italy

Supporting Information

ABSTRACT: The heterobimetallic complexes, (η^5-indenyl)[1-$Me_2Si(^tBuN)TiCl_2$]-3-C_nH_{2n}-[*N*,*N*-bis(2-(ethylthio)ethyl)-amine]$CrCl_3$ (n = 0, **Ti-C_0-Cr^{SNS}**; n = 2, **Ti-C_2-Cr^{SNS}**; n = 6, **Ti-C_6-Cr^{SNS}**), (η^5-indenyl)[1-$Me_2Si(^tBuN)TiCl_2$]-3-C_2H_4-[*N*,*N*-bis-((o-OMe-C_6H_4)$_2$P)amine]$CrCl_3$ (**Ti-C_2-Cr^{PNP}**), and (η^5-indenyl)[1-$Me_2Si(^tBuN)TiCl_2$]-3-C_2H_4-[*N*,*N*-bis((diethylamine)-ethyl)-amine]$CrCl_3$ (**Ti-C_2-Cr^{NNN}**), are synthesized, fully characterized, and employed as olefin polymerization catalysts. With ethylene as the feed and MAO as cocatalyst/activator, SNS-based complexes **Ti-C_0-Cr^{SNS}**, **Ti-C_2-Cr^{SNS}**, and **Ti-C_6-Cr^{SNS}** afford linear low-density polyethylenes (LLDPEs) with exclusive *n*-butyl branches (6.8−25.8 branches/1000 C), while under identical polymerization conditions **Ti-C_2-Cr^{PNP}** and **Ti-C_2-Cr^{NNN}** produce polyethylenes with heterogeneous branching (C_2, C_4, and $C_{\geq 6}$) or negligible branching, respectively. Under identical ethylene polymerization conditions, **Ti-C_0-Cr^{SNS}** produces polyethylenes with higher activity (4.5× and 6.1×, respectively), M_n (1.3× and 1.8×, respectively), and branch density (1.4× and 3.8×, respectively), than **Ti-C_2-Cr^{SNS}** and **Ti-C_6-Cr^{SNS}**. Versus a **CGC^{Et}Ti** + **SNSCr** tandem catalyst, **Ti-C_0-Cr^{SNS}** yields polyethylene with somewhat lower activity, but with 22.6× higher M_n and 4.0× greater branching density under identical conditions. In ethylene +1-pentene competition experiments, **Ti-C_0-Cr^{SNS}** yields 5.5% *n*-propyl branches and 94.5% *n*-butyl branches at [1-pentene] = 0.1 M, and the estimated effective local concentration of 1-hexene is ∼8.6 M. In contrast, the tandem **CGC^{Et}Ti** + **SNSCr** system yields 91.0% *n*-propyl branches under identical reaction conditions. The homopolymerization and 1-pentene competition results argue that close Ti···Cr spatial proximity together with weak C-H···Ti and C-H···S interactions significantly influence relative 1-hexene enchainment and chain transfer rates, supported by DFT computation, and that such effects are conversion insensitive but cocatalyst and solvent sensitive.

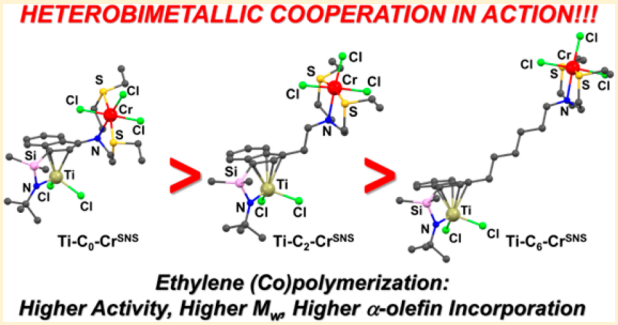

1. INTRODUCTION

Much research in homogeneous multimetallic catalysis focuses on mimicking the cooperative properties of enzymes[1] in the quest for more efficient/selective catalytic transformations (e.g., urease,[2] alkaline phosphatase;[3] Chart 1). Many metalloenzymes containing two or more metal centers mediate the cooperative binding, activation, and conversion of otherwise challenging substrates, due to conformational control, high local reagent concentrations, and preorganization of reactive species.[5] Similarly, solution-phase abiotic multimetallic cooperative catalysis has advanced over the past decade,[6] with impressive examples of homo- and heteronuclear complexes cooperatively activating both reagents in bimolecular reactions, overcoming entropic constraints, and recognizing functional groups and/or prochiral faces.[6c] This strategy has been applied in a variety of catalytic transformations, including epoxidations,[7] olefin hydrogenation and hydroformylation,[6b] and coordinative polymerizations (Chart 1).[8] Regarding single-site olefin polymerization catalysis,[9] we previously identified distinctive (metal center)···(metal center) cooperative effects in covalently linked, homobimetallic group 4 **C_n-CGC^2-M_2**, M = Ti, Zr; n = 1, 2 constrained geometry[10,11] as well as group 4 **FI^2-M_2**, (M = Ti, Zr)[12] and group 10 **FI^2-Ni_2** phenoxyiminato olefin polymerization catalysts.[13,14] Both homobimetallic catalyst families exhibit remarkably enhanced polyethylene M_ns, chain branching, and comonomer enchainment selectivity versus the monometallic counterparts **CGC-M**, **FI-M** (M = Ti, Zr), and **FI-Ni**, respectively. A complementary approach to covalently and electrostatically linked[15] bimetallic catalysts is tandem olefin polymerization catalysis.[16] Here, mixtures of oligomerization + polymerization catalysts have attracted attention since they economically utilize ethylene as the only feed.[17] However, tandem catalytic systems confront multiple issues: (1) the efficiency of elimination + intermolecular enchainment sequences is challenged at low catalyst concentrations; and (2) α-olefin incorporation is sensitive to the conversion time. A different strategy which in principle offers far greater catalyst structural and stoichiometry control over the polymerization process, but which is synthetically more challenging, imple-

Received: May 16, 2014
Published: July 1, 2014

 © 2014 American Chemical Society dx.doi.org/10.1021/ja5046742 | J. Am. Chem. Soc. 2014, 136, 10460−10469

Chart 1. (A) Examples of Enzymatic Catalysis and (B) Selected Examples of Abiotic Multimetallic Catalysts[4]

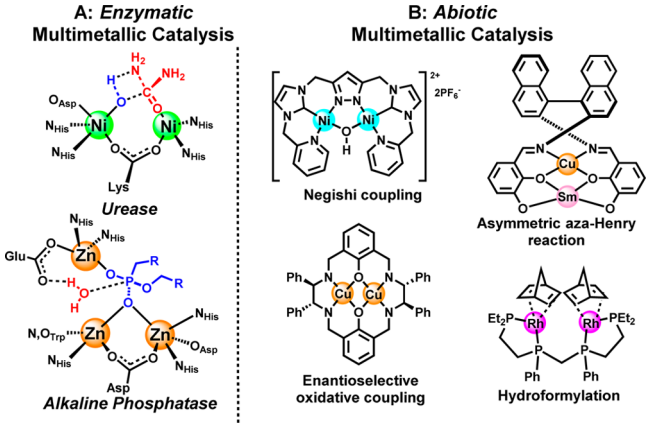

Chart 2. Heterobimetallic Olefin Polymerization Precatalyst and Mononuclear Building Blocks

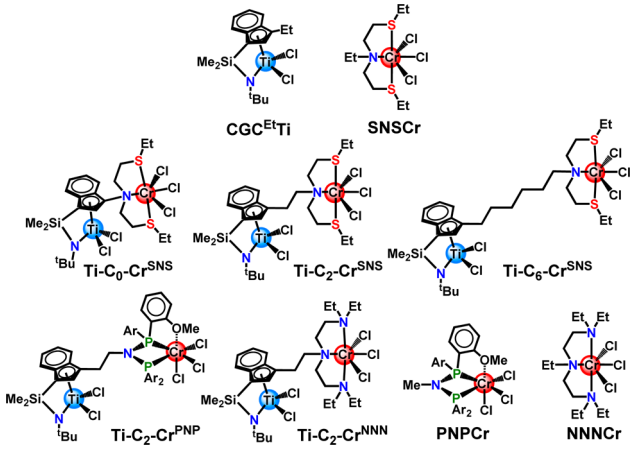

ments covalently joined heterobinuclear catalysts.[18] In the most striking example to date,[19] complex **Ti-C_2-Cr^{SNS}** (Chart 2), a very active Ti constrained geometry olefin polymerization/copolymerization catalyst[10a] (**$CGC^{Et}Ti$**, Chart 2) is paired with an ethylene trimerization selective[20] bis(thioether)amine Cr(III) catalyst **SNSCr** (Chart 2).[21] The individual metal centers exhibit two distinctly different mechanisms for olefin polymerization/copolymerization (Ti center) and ethylene trimerization (Cr center): chain propagation and transfer at Ti follow classic single-site propagation and chain transfer pathways,[22,23] while 1-hexene formation at Cr takes place via oxidative-addition/reductive-elimination sequences and a metallacycloheptane.[24] Importantly, with ethylene as the only feed, **Ti-C_2-Cr^{SNS}** was shown to produce LLDPE with M_ws as high as 460 kg·mol^{-1} and exclusively *n*-butyl branches in conversion-insensitive densities of ∼18 branches/1000 carbon atoms, which are SNSCr mixture (conversion dependent) under achieved by tandem mononuclear **$CGC^{Et}Ti$ + SNSCr** mixtures under identical reaction conditions. Interestingly, the previous studies of homobimetallic group 4 CGC catalysts suggest that the magnitude of cooperative effects, as indexed by product M_w and comonomer enchainment selectivity, roughly scales inversely with metal···metal distance.[8a] This raises the intriguing question of whether and in what way **Ti-C_n-Cr^{SNS}** mediated cooperative enchainment effects might vary, if at all, with group 4 metal···group 6 metal proximity.

Here we report the synthesis and full characterization of a series of **Ti-C_n-Cr^{SNS}** catalysts where the bridge length *n* is varied from 0 to 2 to 6 (Chart 2). In ethylene homopolymerization experiments it will be seen that enchainment cooperativity and the ability of exogenous 1-pentene to compete with 1-hexane for enchainment vary dramatically with bridge length, with the *n* = 0 heterobimetallic catalyst achieving almost complete 1-pentene exclusion. Homopolymerization, copolymerization, and DFT computational results argue that accessible Ti···Cr proximity significantly influences chain transfer rates and selectivity for 1-hexene enchainment in a mechanistically understandable way and that such effects are both cocatalyst and solvent sensitive. In addition, **Ti-C_2-Cr^{PNP}** and **Ti-C_2-Cr^{NNN}** (Chart 2) having different Cr ligation (PNP = (*o*-MeO-C_6H_4)$_2$PN(Me)P(*o*-MeO-C_6H_4)$_2$],[25] NNN = [(C_2H_5)$_2$-N-C_2H_5-]$_2$N(Et)[26]) are synthesized and characterized. Ethylene homopolymerization experiments reveal that **Ti-C_2-Cr^{PNP}** produces LLDPE with heterogeneous branching, while **Ti-C_2-Cr^{NNN}** yields exclusively linear polyethylene.

2. RESULTS

The goal of this investigation is to investigate the scope and mechanism of cooperative enchainment effects between two mechanistically dissimilar yet proximate active catalytic centers, exploring the metrics of polyethylene chain branch densities and molecular masses. First, the synthesis and structural characterization of three Ti/Cr catalysts (**Ti-C_n-Cr^{SNS}**, *n* = 0, 2, 6) covalently linked by a -C_nH_{2n}- bridge are described. Second, the effects of varying the metal···metal proximity on the ethylene homopolymerization phenomenology are explored, including proximity effects on the activity, branch type and density, polymer molecular mass, and competing comonomer enchainment. This mechanistic information is further interpreted with DFT computation. Third, the effects of different cocatalyst and polar solvents on ethylene polymerization are discussed. Finally, **Ti-C_2-Cr^{PNP}** and **Ti-C_2-Cr^{NNN}** are also synthesized and investigated for ligand framework effects on enchainment cooperativity.

2.1. Synthesis of Binuclear Ligands. The syntheses of ligands **H_2CGC-C_0-SNS**, **H_2CGC-C_2-SNS**, and **H_2CGC-C_6-SNS** employ different reaction pathways. Intermediate 3-[($EtSCH_2CH_2$)$_2$N]-indene (**1**), for the synthesis of **H_2CGC-C_0-SNS**, is obtained by reaction of 1-indanone with *N*,*N*-bis(2-(ethylthio)ethyl)amine in refluxing toluene using a Dean−Stark trap (Scheme 1). In contrast, binuclear ligands **H_2CGC-C_2-SNS** and **H_2CGC-C_6-SNS** are prepared by the route outlined in Scheme 1. Here 3-ethylamine-indene and 3-hexylamine-indene are produced by the salt elimination reaction of lithium indenide with 3-bromoethylamine and 6-bromohexylamine, respectively. Condensations of 3-ethylamine-indene hydrobromide or 3-hexylamine-indene hydrobromide with 2.0 equiv of 1-bromo-2-(ethylthio)ethane yields 3-[($EtSCH_2CH_2$)$_2$NC_2H_4]-indene (**2**) or 3-[($EtSCH_2CH_2$)$_2$NC_6H_{12}]-indene (**3**). The oily binuclear ligands **H_2CGC-C_0-SNS**, **H_2CGC-C_2-SNS**, and **H_2CGC-C_6H_{12}-SNS** are then produced by ^{n}BuLi deprotonation of indene derivatives **1**, **2**, and **3**, respectively, followed by sequential addition of Me_2SiCl_2 and ^{t}BuNH$_2$. The reactions proceed in high yield and afford products of high purity, as confirmed by conventional spectroscopic and analytical methodologies. The ligands **H_2CGC-C_2-PNP** and **H_2CGC-C_2-NNN** were prepared in high yield via a methodology similar to that used for **H_2CGC-C_2-SNS** (Scheme S1) and were

dx.doi.org/10.1021/ja5046742 | J. Am. Chem. Soc. 2014, 136, 10460−10469

Scheme 1. Synthesis of Ligands H_2CGC-C_0-SNS, H_2CGC-C_2-SNS, and H_2CGC-C_6-SNS and Heterobimetallic Complexes Ti-C_0-Cr^{SNS}, Ti-C_2-Cr^{SNS}, and Ti-C_6-Cr^{SNS}[a]

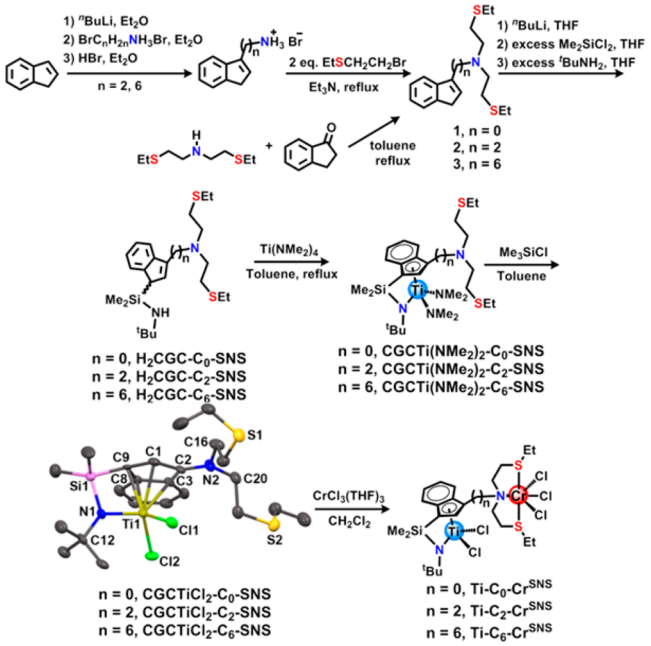

[a]Molecular structure of **CGCTiCl$_2$-C$_0$-SNS**. Thermal Ellipsoids are drawn at the 50% probability level. H atoms are omitted for clarity.

characterized by standard spectroscopic and analytical techniques.

2.2. Synthesis of Heterobimetallic Complexes. Ti-C_0-Cr^{SNS}, Ti-C_2-Cr^{SNS}, and Ti-C_6-Cr^{SNS} are synthesized as outlined in Scheme 1. The first step is the synthesis of monometallic titanium amido complexes **CGCTi(NMe$_2$)$_2$-C$_0$-SNS**, **CGCTi(NMe$_2$)$_2$-C$_2$-SNS**, and **CGCTi(NMe$_2$)$_2$-C$_6$-SNS** via protodeamination of Ti(NMe$_2$)$_4$ with the free ligands **H_2CGC-C$_0$-SNS**, **H_2CGC-C$_2$-SNS**, and **H_2CGC-C$_6$-SNS**, respectively, in refluxing toluene with continuous removal of the volatile HNMe$_2$ byproduct. The shortest reaction time is required for the metalation of **CGCTi(NMe$_2$)$_2$-C$_6$-SNS** (1−2 days), while longer reaction times (5−10 days) are needed for **CGCTi(NMe$_2$)$_2$-C$_2$-SNS** and **CGCTi(NMe$_2$)$_2$-C$_0$-SNS**, likely due to differing steric restraints. Next, reaction of the Ti amido complexes with excess Me$_3$SiCl affords the monometallic complexes **CGCTiCl$_2$-C$_0$-SNS**, **CGCTiCl$_2$-C$_2$-SNS**, and **CGCTiCl$_2$-C$_6$-SNS**, which are purified by recrystallization from pentane and characterized by standard techniques. Subsequent overnight reaction of these complexes with $CrCl_3(THF)_3$ in CH_2Cl_2 affords paramagnetic **Ti-C$_0$-Cr^{SNS}**, **Ti-C$_2$-Cr^{SNS}**, and **Ti-C$_6$-Cr^{SNS}** (Scheme 1), the constitutions of which are confirmed by elemental analysis (Ti, Cr, C, H, N), ^{1}H NMR spectroscopy (very broad), and MALDI-TOF MS. All attempts to grow **Ti-C$_n$-Cr^{SNS}** crystals suitable for diffraction studies yielded mixtures of uninformative byproducts, probably due to the instability of the Cr center in the particular crystallization solvents over prolonged times. In contrast, the heterobimetallic Ti-Cr complexes are stable in the solid state and under polymerization conditions (*vide infra*). High-resolution MALDI-TOF using **Ti-C$_0$-Cr^{SNS}**, **Ti-C$_2$-Cr^{SNS}**, and **Ti-C$_6$-Cr^{SNS}** NALDI targets clearly reveals molecular parent ion patterns corresponding to the [**Ti-C$_0$-Cr^{SNS}H**]$^+$, [**Ti-C$_2$-Cr^{SNS}H**]$^+$, and [**Ti-C$_6$-Cr^{SNS}H**]$^+$ cations. Bimetallic complexes **Ti-C$_2$-Cr^{PNP}** and **Ti-C$_2$-Cr^{NNN}** are synthesized by methodology similar to that for **Ti-C$_2$-Cr^{SNS}** (see Supporting Information). All bimetallic complexes exhibit good stability in moderately coordinating solvents, as confirmed by ^{1}H NMR in THF-d_8, where the $CrCl_3$ moiety is not displaced (*vide infra*).

DFT geometry optimizations for all three heterobimetallic precatalysts were carried out to determine the average proximities between the Ti and the Cr centers (Figure S3), which are found to be 6.0 Å for **Ti-C$_0$-Cr^{SNS}**, 8.1 Å for **Ti-C$_2$-Cr^{SNS}**, and 13.2 Å for **Ti-C$_6$-Cr^{SNS}**. Comparison of the geometrical parameters and charge distributions for **Ti-C$_0$-Cr^{SNS}**, **Ti-C$_2$-Cr^{SNS}**, and **Ti-C$_6$-Cr^{SNS}** shows interesting proximity effects on the Ti coordination. Thus, different distance distributions between the Ti center and the C atoms of the Cp fragment are observed for **Ti-C$_0$-Cr^{SNS}** versus **Ti-C$_2$-Cr^{SNS}** and **Ti-C$_6$-Cr^{SNS}** as a consequence of differing coordination characteristics (Table S3) and implying η^3 coordination for **Ti-C$_0$-Cr^{SNS}** versus η^5 for **Ti-C$_2$-Cr^{SNS}** and **Ti-C$_6$-Cr^{SNS}**. These results are in excellent agreement with the experimental diffraction data for **CGCTiCl$_2$-C$_0$-SNS** and **CGCTiCl$_2$-C$_2$-SNS** (See Supporting Information). The different coordination types can be ascribed both to metal center−metal center steric repulsion and the electronic effects of the SNS nitrogen bond to the indenyl ring.

Table 1. Ethylene Polymerization Data for CGC^{Et}Ti, SNSCr, CGCTiCl$_2$-C$_0$-SNS, CGCTiCl$_2$-C$_2$-SNS, CGCTiCl$_2$-C$_6$-SNS, CGC^{Et}Ti + SNSCr, Ti-C$_0$-Cr^{SNS}, Ti-C$_2$-Cr^{SNS}, and Ti-C$_6$-Cr^{SNS}[a]

entry	catalyst	PE (g)	activity[b] (PE)	oligomers[c] (g)	activity[d] (oligomers)	ρ_{br}[e]	M_w[f] (kg·mol^{-1})	M_n[f] (kg·mol^{-1})	PDI[f]	T_m[g] (°C)
1	**CGC^{Et}Ti**	6.500	975.0	–	–	0	42	16.8	2.5	128.4
2	**SNSCr**	0.045	6.7	0.490	73.5	0	144	65.3	2.2	133.6
3	**CGCTiCl$_2$-C$_0$-SNS**	0.165	24.7	–	–	0	165	78.5	2.1	137.6
4	**CGCTiCl$_2$-C$_2$-SNS**	0.054	8.1	–	–	0	77	24.0	3.2	136.8
5	**CGCTiCl$_2$-C$_6$-SNS**	0.077	11.5	–	–	0	64	40.0	1.6	132.0
6	**CGC^{Et}Ti + SNSCr**	3.200	480.0	0.204	30.6	6.4	26	11.4	2.3	125.9
7	**Ti-C$_0$-Cr^{SNS}**	0.820	123.0	0.491	73.7	25.8	593	237	2.5	123.9
8	**Ti-C$_2$-Cr^{SNS}**	0.184	27.6	0.075	11.3	18.2	461	184	2.5	123.5
9	**Ti-C$_6$-Cr^{SNS}**	0.134	20.1	0.066	9.9	6.8	319	127	2.5	126.0

[a][Catalyst] = 10 μmol of **CGC^{Et}Ti**; 10 μmol of **SNSCr**; 10 μmol of **CGC^{Et}Ti** + 10 μmol of **SNSCr**; 10 μmol of **CGCTiCl$_2$-C$_0$-SNS**, **CGCTiCl$_2$-C$_2$-SNS**, **CGCTiCl$_2$-C$_6$-SNS**, **Ti-C$_0$-Cr^{SNS}**, **Ti-C$_2$-Cr^{SNS}**, and **Ti-C$_6$-Cr^{SNS}**, MAO/catalyst =500, 50 mL toluene, 5 min, 80 °C, constant 8 atm ethylene. Entries performed in duplicate. [b]kg (PE)·mol^{-1} (catalyst)·h^{-1}·atm^{-1}. [c]By GC-TOF, mesitylene internal standard. [d]kg (oligomers)·mol^{-1} (catalyst)·h^{-1}·atm^{-1}. [e]Branch density (branches per 1000 C atoms) as determined by ^{13}C NMR analysis.[30] [f]By triple-detection GPC. [g]Melting temperature by DSC.

dx.doi.org/10.1021/ja5046742 | J. Am. Chem. Soc. 2014, 136, 10460−10469

Table 2. Ethylene Polymerization Data as a Function of Polymerization Time at 80 °C for CGC^{Et}Ti + SNSCr and Ti-C$_0$-Cr^{SNS}[a]

entry	catalyst	t (min)	PE (g)	activity[b] (PE)	oligomers[c] (g)	activity[d] (oligomers)	ρ_{br}[e]	M_w[f] (kg·mol^{-1})	M_n[f] (kg·mol^{-1})	PDI[f]	T_m[g] (°C)
1	CGC^{Et}Ti + SNSCr	5	3.200	480.0	0.204	30.6	6.4	26.2	11.4	2.3	125.9
2	CGC^{Et}Ti + SNSCr	10	5.950	446.2	0.382	28.6	8.2	15.3	6.1	2.5	123.2
3	CGC^{Et}Ti + SNSCr	20	10.80	405.0	0.720	27.0	11.8	12.5	5.4	2.3	121.9
4	Ti-C$_0$-Cr^{SNS}	5	0.820	123.0	0.491	73.7	25.8	593	237	2.5	123.9
5	Ti-C$_0$-Cr^{SNS}	10	1.610	121.7	0.930	69.8	26.2	652	233	2.8	123.1
6	Ti-C$_0$-Cr^{SNS}	20	3.040	114.0	1.780	66.7	26.5	795	284	2.8	123.8
7	Ti-C$_0$-Cr^{SNS}	60	6.250	78.1	4.360	54.5	28.7	854	406	2.1	122.7

[a][Catalyst] = 10 μmol of **CGC^{Et}Ti** + 10 μmol of **SNSCr**; 10 μmol of **Ti-C$_0$-Cr^{SNS}**, MAO/catalyst =500, 50 mL toluene, T = 80 °C, P = 8 atm. Entries performed in duplicate. [b]kg (PE)·mol^{-1} (catalyst)·h^{-1}·atm^{-1}. [c]By GC-TOF, mesitylene added as internal standard. [d]kg (oligomers)·mol^{-1} (catalyst)·h^{-1}·atm^{-1}. [e]Branch density (branches per 1000 C atoms) as determined by ^{13}C NMR analysis.[30] [f]By triple detection GPC. [g]Melting temperature by DSC.

2.3. Olefin Polymerization Studies. *2.3.1. Catalytic Center Proximity Effects: Activity and Polymer Molecular Mass.* Ethylene polymerizations were carried out using rigorously anhydrous/anaerobic methodology with attention to exotherm and mass transfer effects.[27] Catalysts were investigated under varied reaction conditions, including cocatalyst/activator MAO/Al ratio (100, 500, 1000), reaction temperature (25, 50, 80, 100 °C), ethylene pressure (1, 3, 5, 8 atm), and reaction time (5, 10, 20, 60 min). Optimum catalytic performance (activity, branches/1000 C, M_n, M_w, PDI, cooperative effects) is achieved with Al: M = 500 at 80 °C under constant 8.0 atm ethylene pressure. Polymerization results are summarized in Tables 1−3. The narrow monomodal polydispersities observed are consistent with well-defined single-site processes.[28] Table 1 entries 6−9 and Figure S36 reveal that ∼22 ×, ∼17× and ∼12× increases in M_n with **Ti-C$_0$-Cr^{SNS}**, **Ti-C$_2$-Cr^{SNS}** and **Ti-C$_6$-Cr^{SNS}**, respectively, vs the mononuclear tandem **CGC^{Et}Ti + SNSCr** system under identical polymerization conditions. For single-site polymerizations, M_n values typically scale as the net rate of chain propagation divided by the net rate of all chain termination processes.[29] In view of the lower activities versus the tandem catalysts, the chain transfer kinetics of the present bimetallic complexes must be substantially depressed to explain the large observed M_n enhancements (*vide infra*). These results in some respects parallel previous results for homobimetallic group 4 CGC catalysts where activities are lower than for the mononuclear analogues, and product M_ns roughly scale inversely with metal···metal distance.[8a] Ethylene homopolymerizations mediated by monometallic **CGC^{Et}Ti** and **CGCTiCl$_2$-C$_0$-SNS**, **CGCTiCl$_2$-C$_2$-SNS**, and **CGCTiCl$_2$-C$_6$-SNS** afford relatively low-M_n/high-melting polyethylenes with negligible chain branching (Table 1 entries 1, 3−5). Note also that the very different polymerization characteristics of the **Ti-C$_n$-Cr^{SNS}** vs **CGCTiCl$_2$-C$_n$-SNS** catalysts (n = 0, 2 and 6; entries 7 vs 3, 8 vs 4, 9 vs 5, Table 1) argue that the -SNSCr center remains intact during the polymerizations. Furthermore, under the present polymerization conditions, the Cr catalysts in either the tandem or bimetallic configurations display good selectivity for ethylene trimerization, ranging from 72% to 99% 1-hexene by NMR spectroscopy and GC-TOF (see distribution in Table S2), with no odd-numbered α-olefins detected by GC-MS, as might arise from chain transfer to MAO. However, under the present experimental conditions, the monometallic **SNSCr** oligomerization catalyst is less selective for 1-hexene (53%) and also produces small amounts (∼9%) of high M_n polyethylene (Table 1, entry 2).[31]

The properties of the polymers produced by **SNSCr** are completely different (M_n, branch density, T_m) from those obtained using the tandem and bimetallic catalysts. Also, although the shorter bridge of **Ti-C$_0$-Cr^{SNS}** would appear to engender greater steric encumbrance, the polymerization activity is found to be ∼4.4× and ∼6.1× greater than that of **Ti-C$_2$-Cr^{SNS}** and **Ti-C$_6$-Cr^{SNS}**, respectively (Table 1, entries 7−9; Figure S36), presumably reflecting both electronic and steric effects.[32] Amine substituents such as on the indenyl of **Ti-C$_0$-Cr^{SNS}** are effective electron donors which can stabilize cationic active centers during polymerization.[33] To compare the stability of the tandem and heterobimetallic catalysts (Table 2), ethylene polymerizations were compared between 5 and 20 min at 80 °C. Activities for both copolymerization and oligomerization versus time reveal that both systems exhibit remarkable stability and similar deactivation characteristics (Figure S34). Note also that the oligomerization activities and 1-hexene selectivity (*vide infra*) do not decline significantly over these times, indicating that Cr center is intact during polymerization.[34]

2.3.2. Catalytic Center Proximity Effects: Chain Transfer/Termination Process. Gel permeation chromatography (GPC) analysis shows that the polymer M_ns (Table 1) increase with decreasing metal···metal distance, in the order: **Ti-C$_6$-Cr^{SNS}** (computed Ti···Cr = 13.2 Å) < **Ti-C$_2$-Cr^{SNS}** (computed Ti···Cr = 8.1 Å) < **Ti-C$_0$-Cr^{SNS}** (computed Ti···Cr = 6.0 Å). These results are consistent with a pathway in which Ti···Cr proximity modifies the catalytic environment and substantially depresses overall termination rates,[35] in turn enhancing M_n[36] (see more below). Furthermore, the M_ns of the polyethylenes produced by **Ti-C$_0$-Cr^{SNS}** at 80 °C are essentially independent of ethylene pressure over a 1.0−8.0 atm range and Al/M ratio over a 100−1000 range (Table 1, entry 7, and Table 3, entries 1−3, 7, 8). This result argues that β-H transfer from the growing polymer chain to coordinated/activated ethylene (chain transfer to monomer)[37] is the primary chain transfer process and that chain transfer to Al-alkyl is negligible.[23,38] End-group analysis by ^{1}H NMR spectroscopy (Figure 1) reveals that the **Ti-C$_0$-Cr^{SNS}**-derived polyethylenes exhibit predominant vinylene (98%; -CH$_2$CH=CH$_2$) end-group distributions along with small amounts of internal olefin (<2%; -CH$_2$-CH=CH-CH$_2$- + -(CH$_2$)C=CH$_2$- + -CH$_2$-CH=CH-C$_4$H$_9$), consistent with the aforementioned chain termination process by chain transfer to monomer rather than chain transfer to Al-alkyl. Interestingly, C=C migration/isomerization[39] is almost negligible for the heterobimetallic catalysts but is substantial for the tandem

dx.doi.org/10.1021/ja5046742 | J. Am. Chem. Soc. 2014, 136, 10460−10469

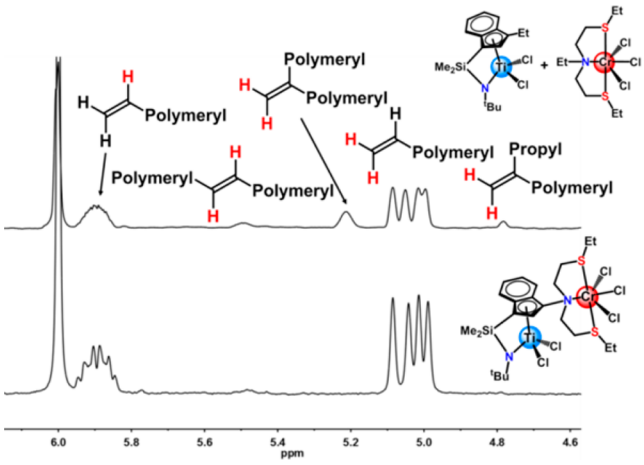

Figure 1. ^{1}H NMR comparison of the end-group regions (δ 6.10−4.60 ppm) of the polyethylenes produced by the **CGC^{Et}Ti + SNSCr** and heterobimetallic **Ti-C$_0$-Cr^{SNS}** catalysts (Table 1, entries 6 and 7, respectively). Spectral intensities are normalized to the polyethylene backbone CH_2 resonance.

system (23%, Figure 1), presumably reflecting steric and/or electronic constraints.

2.3.3. Catalytic Center Proximity Effects: Branch Type and Density. ^{13}C NMR spectra of the polyethylenes produced by **CGC^{Et}Ti + SNSCr**, **Ti-C$_0$-Cr^{SNS}**, **Ti-C$_2$-Cr^{SNS}**, and **Ti-C$_6$-Cr^{SNS}** are depicted in Figure S33 along with assignments for the polymer skeletal positions. Note that the branch density in the polyethylene chains is significantly enhanced as the bridge length is shortened (Figure 2): **Ti-C$_0$-Cr^{SNS}** yields the

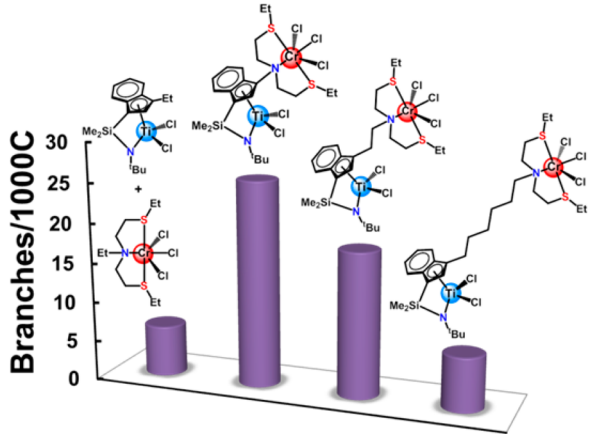

Figure 2. Branches/1000 C in the polyethylenes produced by the **CGC^{Et}Ti + SNSCr**, **Ti-C$_0$-Cr^{SNS}**, **Ti-C$_2$-Cr^{SNS}** and **Ti-C$_6$-Cr^{SNS}** catalysts (Table 1, entries 6−9) under identical reaction conditions at 80 °C.

maximum branch density of 25.8 *n*-butyl branches/1000 C atoms, with branches of any other length <1%, while **Ti-C$_2$-Cr^{SNS}** affords polyethylenes having a branch density of 18.2 *n*-butyl branches/1000 C atoms. Interesting, the **Ti-C$_6$-Cr^{SNS}** catalyst introduces only 6.8 *n*-butyl branches/1000 C atoms, which is similar to the **CGC^{Et}Ti + SNSCr** tandem catalytic system, 6.4 *n*-butyl branches/1000 C atoms, suggesting a similar comonomer enchainment pathway. These results are consistent with a picture in which greater Ti···Cr proximity/cooperation enhances 1-hexene co-enchainment in the ethylene polymerization process. Note from Table 2 entries 4−6 and Figure S35 that the polyethylene branch type and density are essentially independent of reaction time/conversion at 80 °C, despite increasing concentrations of available "free" oligomer. This result is similar to that for **Ti-C$_2$-Cr^{SNS}** and stands in contrast to the results for the tandem **CGC^{Et}Ti + SNSCr** system. Note that while increasing "free" oligomer concentrations/longer reaction times depress copolymer M_ns and activities in the tandem system (typical of single-site CGCTi catalysts where comonomer enchainment is sterically sensitive and chain transfer to monomer dominates),[40] they have less effect on the heterobimetallic catalysts. The proximate tethered SNSCr oligomerization center clearly alters the pathway by which 1-hexene is created/enchained and, perhaps, by which chain transfer occurs, versus that in mononuclear CGCTi. The result for **Ti-C$_0$-Cr^{SNS}** is higher M_n copolymers with higher densities of *n*-Bu-only branching.

For **Ti-C$_0$-Cr^{SNS}** from 25 to 80 °C (Table 3), the activity of the Cr oligomerization center (total oligomerization product mass) increases by ∼22×, while the total Ti-centered polymerization activity increases by ∼4× (Figure S37). This implies that the Cr- and Ti-centered processes in **Ti-C$_0$-Cr^{SNS}** have different activation energetics and that 1-hexene enchainment within this assembly is constrained/gated in such a way that while some additional 1-hexene is enchained at higher temperatures, the excess "leaks out" rather than being incorporated in product polymer. In accord with this selectivity picture, note also in Table 3 entries 1−3 that the branch density is rather insensitive to the ethylene pressure. These same entries indicate, as already noted above, that M_n is insensitive to ethylene pressure, suggesting that chain transfer to monomer is the major growth termination mode.[37] Note also that at 100 °C, the branch density is similar to that at 80 °C (25.2/1000 C vs 25.8/1000 C, respectively) at the same ethylene pressure (8 atm) even though the polymerization activity remains high, suggesting that the 1-hexene enchainment rate may saturate at higher temperatures with the rate lawing tending to zero-order in [α-olefin].[41]

2.3.4. DFT Analysis of Structure and Reaction Energetics. To understand how metal proximity enhances polyethylene M_n with the bimetallic catalysts and qualitatively explain the experimental trends, a comparison between propagation and termination energetic paths for mononuclear **CGC^{Et}Ti** and binuclear **Ti-C$_0$-Cr^{SNS}** was carried out. Since the starting point for both the propagation and termination pathways is the π-complex (Scheme 2), counteranion effects can be assumed to remain constant in this first level of analysis (see Supporting Information). The initial enchainment and chain transfer processes involve conventional Ti-ethylene π-complex formation (Scheme 2) at both the mono and binuclear catalysts. The insertion transition state in both cases involves ethylene monomer approach to form a coplanar four-center (Ti-C1-C2-C3) bonding framework (Scheme 2). The elongation of one C3-H bond (to 1.12 and 1.14 Å) and distortion of the Ti-C3-H angle (to 96.6 and 81.6°) from tetrahedral (109.5°) indicate α-agostic interactions that stabilize/preorganize the overall insertion process.

In the chain transfer transition states, concerted bond-forming/-breaking, paralleling H transfer, is active between Ti and atoms C1/C3, respectively (Scheme 2). At this point, the C1-C2 and C3-C4 bond lengths are intermediate between single and double bonds. In both mononuclear and bimetallic catalysts, the computed C4-H and C2-H distances lie close to 1.47 Å, indicating a symmetrical H transfer process. The chain

dx.doi.org/10.1021/ja5046742 | J. Am. Chem. Soc. 2014, 136, 10460−10469

Table 3. Effects of Pressure and Temperature on Ethylene Polymerization by Ti-C_0-Cr^{SNS}[a]

entry	P (atm)	T (°C)	PE (g)	activity[b] (PE)	oligomers[c] (g)	activity[d] (oligomers)	ρ_{br}[e]	M_w[f] (kg·mol^{-1})	M_n[f] (kg·mol^{-1})	PDI[f]	T_m[g] (°C)
1	1	80	0.056	67.2	0.035	42.0	17.4	633	264	2.4	124.5
2	3	80	0.290	116.0	0.145	58.0	18.2	606	189	3.2	126.1
3	5	80	0.495	118.8	0.270	64.8	23.4	656	226	2.9	121.8
4	8	25	0.205	30.7	0.022	3.3	10.2	643	268	2.4	126.9
5	8	50	0.335	50.2	0.210	31.5	17.6	597	186	3.2	123.3
6	8	100	0.774	116.1	0.498	74.7	25.2	493	205	2.4	123.7
7[h]	8	80	0.203	30.4	0.015	2.2	5.6	591	227	2.6	126.0
8[i]	8	80	0.825	123.7	0.520	78.0	21.2	567	236	2.4	126.9

[a][Catalyst] = 10 μmol of **Ti-C_0-Cr^{SNS}**, MAO/catalyst =500, 50 mL toluene, time =5 min. Entries performed in duplicate. [b]kg (PE)·mol^{-1} (catalyst)·h^{-1}·atm^{-1}. [c]By GC-TOF, mesitylene added as internal standard. [d]kg (oligomers)·mol^{-1} (catalyst)·h^{-1}·atm^{-1}. [e]Branch density (branches per 1000 C atoms) as determined by ^{13}C NMR analysis.[30] [f]By triple detection GPC. [g]Melting temperature by DSC. [h]MAO/catalyst =100. [i]MAO/catalyst =1000.

Scheme 2. Ti-Centered Propagation and Chain Transfer Steps in Olefin Polymerization Processes at Mononuclear $CGC^{Et}Ti$ and Binuclear Ti-C_0-Cr^{SNS} Catalysts

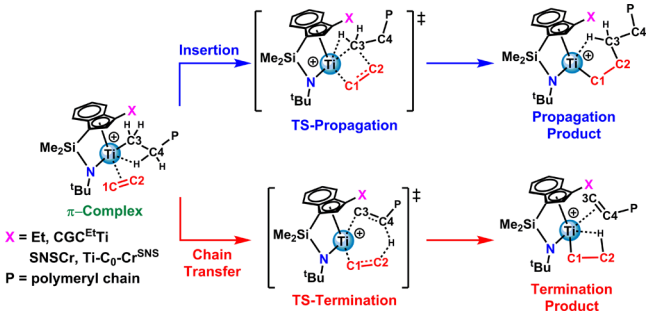

transfer process leads to a linear alkene (here propene) coordinated to the Ti center and an ethyl fragment σ-bonded to Ti (Scheme 2). β-agostic interactions are active between the ethyl fragment and Ti. This analysis also reveals that the Cr catalyst proximity in **Ti-C_0-Cr^{SNS}** stabilizes the insertive transition state and product as well as the β-H chain transfer transition state and product at Ti versus the mononuclear **$CGC^{Et}Ti$** catalyst (Figure 3). Note that stabilization of the propagation transition state is greater than for the termination transition state (Figure 3); the energetic difference is 3.3 kcal/mol for the **$CGC^{Et}Ti$** and 5.0 kcal/mol for **Ti-C_0-Cr^{SNS}**. Since M_n should scale as the propagation rate/chain transfer rate, these results are in good accord with the increased polyethylene M_ns achieved with the bimetallic catalysts (Tables 1, entries 6 and 7). To obtain better insight into the α-olefin coenchainment mechanism, calculations next focused on the catalytic differences between **Ti-C_0-Cr^{SNS}** and **Ti-C_2-Cr^{SNS}**. Questions concern the role of agostic interactions[42] in comonomer activation/enchainment and the differences in polymerization characteristics between **Ti-C_0-Cr^{SNS}** and **Ti-C_2-Cr^{SNS}**. Figures 4A and B show the optimized structures of the **Ti-C_0-Cr^{SNS}** and **Ti-C_2-Cr^{SNS}** active catalysts in which a 1-hexene molecule interacts simultaneously with two metal centers. Note that in both **Ti-C_0-Cr^{SNS}** and **Ti-C_2-Cr^{SNS}** a π-interaction occurs between the C=C bond and the Cr while the Ti center is involved in agostic C(sp^3)-H binding. These latter interactions are evidenced by the elongation of one C(5)-H_2 bond (1.13 Å) in **Ti-C_0-Cr^{SNS}** and one C(6)-H_3 bond (1.12 Å) in **Ti-C_2-Cr^{SNS}** with respect to a standard sp^3 C-H bond distance (1.10 Å). Note that the agostic interaction involves the 1-hexene C5 with **Ti-C_0-Cr^{SNS}** and C6 for **Ti-C_0-Cr^{SNS}**, tracking the different computed Ti···Cr distances for **Ti-C_0-Cr^{SNS}** (4.67 Å) and **Ti-C_2-Cr^{SNS}** (6.34 Å). The greater computed C-H distance of 1.13 Å for **Ti-C_0-Cr^{SNS}** vs 1.12 Å for **Ti-C_2-Cr^{SNS}** as well as the smaller Ti···H distance in **Ti-C_0-Cr^{SNS}** (2.11 Å) vs **Ti-C_2-Cr^{SNS}** (2.17 Å) likely reflect stronger **Ti-C_0-Cr^{SNS}** agostic bonding. Interestingly, the NBO population analysis also reveals further weak interactions for **Ti-C_0-Cr^{SNS}** between Cr–S1[43] and Ti. Specifically, in addition to the C-H sp^3 agostic donation to a Ti empty orbital (mostly p in character) which is also seen in **Ti-C_2-Cr^{SNS}**, a slightly stabilizing electronic donation involving a C-H sp^3 orbital and an empty, diffuse S-Cr antibonding orbital.

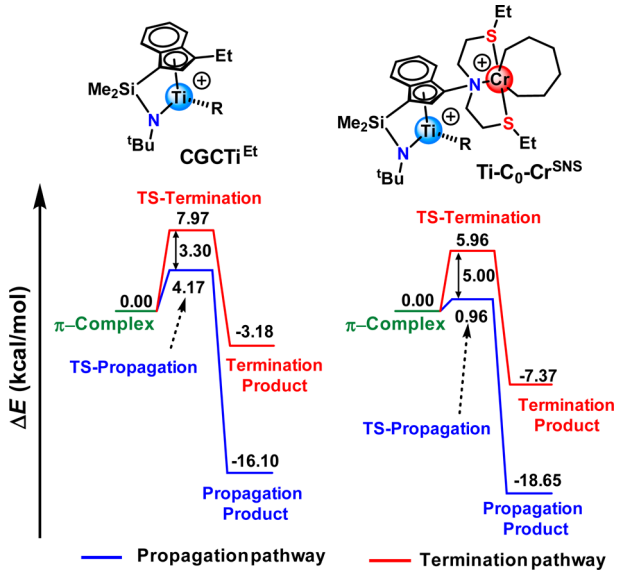

Figure 3. Energetic profiles (kcal/mol) for propagation (blue) and termination (chain transfer; red) pathways for ethylene homopolymerization at Ti catalyzed by mononuclear and binuclear catalysts.

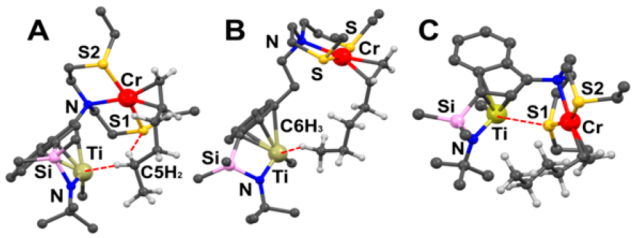

Figure 4. Computed 1-hexene binding by the activated cationic heterobimetallic catalysts (A) **Ti-C_0-Cr^{SNS}**, (B) **Ti-C_2-Cr^{SNS}**, and (C) the hemilabile weak Ti···S interaction. Weak Interactions are shown as red dotted lines.

dx.doi.org/10.1021/ja5046742 | J. Am. Chem. Soc. 2014, 136, 10460–10469

Table 4. Ethylene +1-Pentene Copolymerization Data Mediated by CGC^{Et}Ti + SNSCr, Ti-C$_0$-Cr^{SNS}, Ti-C$_2$-Cr^{SNS}, and Ti-C$_6$-Cr^{SNS} Catalysts[a]

entry	catalyst	[1-pentene]	PE (g)	activity[b]	$\rho_{n\text{-propyl}}$[c]	$\rho_{n\text{-butyl}}$[c]	% *n*-propyl	M_w[d] (kg·mol^{-1})	M_n[d] (kg·mol^{-1})	PDI[d]	T_m[e] (°C)
1	CGC^{Et}Ti + SNSCr	0.1 M	2.850	427.5	61.9	6.1	91.0	33.4	15.2	2.2	110.9
2	Ti-C$_0$-Cr^{SNS}	0.1 M	0.782	117	1.4	23.9	5.5	554	205	2.7	121.9
3	Ti-C$_0$-Cr^{SNS}	0.5 M	0.585	87.8	1.7	22.2	7.1	551	196	2.8	118.6
4	Ti-C$_0$-Cr^{SNS}	1.0 M	0.450	67.5	2.4	21.0	10.2	349	174	2.0	118.3
5	Ti-C$_2$-Cr^{SNS}	0.1 M	0.170	25.8	9.3	17.4	34.8	606	242	2.5	115.0
6	Ti-C$_6$-Cr^{SNS}	0.1 M	0.092	13.8	7.0	5.7	55.1	186	84.5	2.2	114.3

[a][Catalyst] = 10 μmol of **CGC^{Et}Ti** + 10 μmol of **SNSCr**; 10 μmol of **Ti-C$_0$-Cr^{SNS}**, **Ti-C$_2$-Cr^{SNS}**, and **Ti-C$_6$-Cr^{SNS}**, MAO/catalyst =500, 50 mL toluene, 5 min, 80 °C, at constant 8 atm ethylene. Entries performed in duplicate. [b]kg (PE)·mol^{-1} (catalyst)·h^{-1}·atm^{-1}. [c]Branch density (branches per 1000 C atoms) by ^{13}C NMR.[30] [d]By triple detection GPC. [e]Melting temperature by DSC.

This interaction is supported by elongation of the Cr−S1 bond (2.44 Å) vs Cr−S2 (2.41 Å). Similar X-H···S interactions (X = C, N) play significant roles in enzymatic reactions, abiotic homogeneous catalysis, and supramolecular materials.[44] In the present case, slight stabilization by Cr d_{z^2} donation to an empty, predominantly Ti orbital is observed. All these interactions further stabilize the 1-hexene-bimetallic binding, doubtless benefiting from the greater Ti···Cr proximity in the **Ti-C$_0$-Cr^{SNS}** framework. Note that for **Ti-C$_0$-Cr^{SNS}**, another stable structure is located when the 1-hexene···Ti agostic interaction is computationally removed. Here the S1 atom approaches the Ti cation, driven by the Ti unsaturation (Figure 4C). Moreover, the NBO analysis reveals strong stabilizing electron donation of a S1 lone pair to an empty Ti orbital. As with the aforementioned agostic interactions, this hemilabile[45] S1−Ti interaction also constrains the intermetallic distances and keeps 1-hexene proximate to the Ti center.

2.3.5. Comonomer Competition Experiments. To better understand the degree to which the trimerization and enchainment processes are concerted in the **Ti-C$_n$-Cr^{SNS}** environment (i.e., is the 1-hexene exclusively endogenous?), competition experiments with added "exogenous" 1-pentene were carried out for both the **CGC^{Et}Ti + SNSCr** tandem catalyst and the heterobimetallic catalysts. Results are compiled in Table 4, and ^{13}C NMR spectra of the four polyethylenes obtained with **CGC^{Et}Ti + SNSCr**, **Ti-C$_0$-Cr^{SNS}**, **Ti-C$_2$-Cr^{SNS}**, and **Ti-C$_6$-Cr^{SNS}** under identical reaction conditions are shown in Figure 5A. Most noteworthy is that the heterobimetallic catalysts produce polyethylenes with *n*-butyl (1-hexene enchainment) densities nearly unchanged from the ethylene-only homopolymerization experiments, while the tandem catalyst yields polyethylenes with far higher *n*-propyl (1-pentene enchainment) branching levels. Note also that **Ti-C$_0$-Cr^{SNS}** with shortest linkage incorporates least *n*-propyl branches, 5.5% of total branches (Table 4, entry 2, Figure 5B), and even at [1-pentene] = 1.0 M.

2.3.6. Cocatalyst and Solvent Effects on Polymerization Processes. Cocatalysts/activators play an enabling role in single-site polymerization processes,[23,38] with $AlR_3/[Ph_3C]^+[B(C_6F_5)_4]^-$ serving as an efficient activator/cocatalyst for both Ti[46] and Cr[47] complexes in olefin polymerization and oligomerization, respectively. Ethylene polymerizations employing the tandem **CGC^{Et}Ti + SNSCr** system and the three heterobimetallic catalysts with $^{i}Bu_3Al/[Ph_3C]^+[B(C_6F_5)_4]^-$ were carried out and the results are summarized in Table S4. Comparing entries 6−9 in Table 1 and entries 1−4 in Table S4, note that $^{i}Bu_3Al/[Ph_3C]^+[B(C_6F_5)_4]^-$ significantly enhances polymerization activity but depresses M_n, suggesting that $^{i}Bu_3Al/[Ph_3C]^+[B(C_6F_5)_4]^-$ has a significantly different activation and ion-pairing characteristics than MAO. Interestingly, the product polymer ^{13}C NMR spectra indicate negligible chain branching, and GC-MS analysis of the liquid phase shows no oligomers. It is known that the selectivity of Cr oligomerization catalysts is highly dependent on ligation,[48] solvent,[49] reaction temperature,[50] and cocatalyst.[47b] In the present case, it is possible that the Cr center is oxidatively deactivated by Ph_3C^+.[51] In addition, the cocatalyst $^{i}Bu_3Al/B(C_6F_5)_3$ was also investigated (Table S4, entries 5, 6)[52] and yields negligible polymer or oligomers. Note also that when MMAO is used as a cocatalyst with **Ti-C$_0$-Cr^{SNS}**, similar polymerization activity is observed, but with significantly lower branch densities versus MAO. These results attest to the sensitivity of the Cr oligomerization characteristics to diverse reagents. Polymerizations in more polar solvents should weaken ion pairing, and compared with polymerizations conducted in toluene (ϵ = 2.38; Table 1, entries 6, 7), more polar C_6H_5Cl (ϵ = 5.68) dramatically increases polymerization activity (Table S4, entries

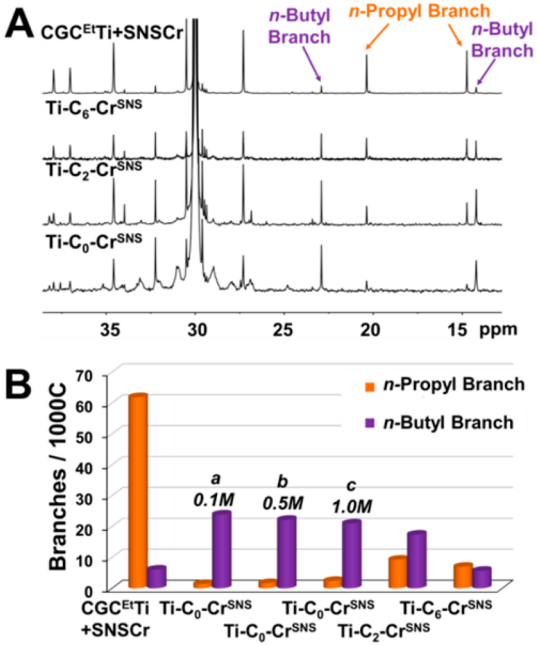

Figure 5. (A) ^{13}C NMR spectra (100 MHz, $C_2D_2Cl_4$, 120 °C) of polyethylenes produced by **CGC^{Et}Ti + SNSCr**, **Ti-C$_6$-Cr^{SNS}**, **Ti-C$_2$-Cr^{SNS}**, and **Ti-C$_0$-Cr^{SNS}** in the presence of 0.1 M 1-pentene (Table 4, entries 1, 2, 5 and 6). Intensities normalized to the polyethylene backbone CH_2 resonance. (B) *n*-propyl and *n*-butyl branches/1000 C in polyethylenes produced by the **CGC^{Et}Ti + SNSCr**, **Ti-C$_0$-Cr^{SNS}**, **Ti-C$_2$-Cr^{SNS}** and **Ti-C$_6$-Cr^{SNS}** catalysts (Table 4, entries 1−6) in the presence of added 1-pentene: *a* = 0.1 M; *b* = 0.5 M; *c* = 1.0 M.

dx.doi.org/10.1021/ja5046742 | J. Am. Chem. Soc. 2014, 136, 10460−10469

9, 10), although there are negligible ethylene solubility differences between toluene and chlorobenzene.[53] In ethylene homopolymerization, **Ti-C_0-Cr^{SNS}** is almost 2× more active in C_6H_5Cl vs toluene. Significantly, however, the product polymer M_ns and branch densities produced by **Ti-C_0-Cr^{SNS}** fall significantly in chlorobenzene versus those in toluene (Table S4, entry 10 vs Table 1, entry 7; 62.3% and 74.8%, respectively); clearly the polymer M_ns and comonomer enchainment selectivity are sensitive to the catalyst-cocatalyst ion pairing, in agreement with previous studies where it was shown that polar solvents weaken catalyst cation−anion electrostatic interactions, enhance the ion-pair structural mobility,[40b] and render the cation "freer" with greater polymerization activity and frequently altered selectivity.[40a] Furthermore, polar solvents may compete for/coordinate with electrophilic metal centers and may weaken/supplant agostic interactions, conceivably yielding lower branch densities.[54] Thus, polar solvents may also alter the transition states for chain transfer processes involving metal···H-C(β) agostic interactions,[55] potentially suppressing cooperative enchainment effects, hence M_n and α-olefin enchainment.

2.3.7. Ligand Structure Effects. In addition to **SNSCr**, ethylene oligomerization catalysts **PNPCr**[56] (Chart 2) and **NNNCr**[57] (Chart 2) are reported to achieve 1-hexene selectivities >97% (for **PNPCr**); among the highest reported to date. Therefore, new bimetallic catalysts **Ti-C_2-Cr^{PNP}** and **Ti-C_2-Cr^{NNN}** were prepared (Scheme S1) for comparison. Under rigorously anhydrous/anaerobic conditions, with attention to exotherm and mass transfer effects, both catalysts are active for ethylene polymerization with MAO as cocatalyst, and results are summarized in Table S5. Under these conditions, **PNPCr** alone exhibits acceptable 1-hexene selectivity (Table S5, entry 2, 99% 1-hexene), while the Cr center in tandem **CGC^{Et}Ti** + **PNPCr** exhibits modest selectivity -- 40.9% 1-hexene in the oligomeric products. Regarding copolymerizations, neither the tandem nor heterobimetallic catalysts are particularly selective for ethylene trimerization, but rather yield a series of linear C_4-C_{22} α-olefins for **Ti-C_2-Cr^{PNP}** (58.5% 1-hexene in the oligomeric product) and no oligomers for **Ti-C_2-Cr^{NNN}**, as confirmed by NMR spectroscopy and GC-MS (Table S5). Thus, the ^{13}C NMR spectrum of the polyethylenes produced by **Ti-C_2-Cr^{PNP}** indicates ethyl, *n*-butyl, and longer *n*-alkyl (≥C6) branches, while the spectrum of those produced by **Ti-C_2-Cr^{NNN}** shows no significant branch resonances.

3. DISCUSSION

3.1. Bimetallic Proximity Effects on Polymerization. In the present strategy, coordinatively "open," highly reactive CGCTi is employed as a "polymer maker", while highly selective and reactive SNSCr is chosen as the "oligomer maker". When the Ti/Cr catalytic centers are covalently linked by a -C_nH_{2n}- bridge (**Ti-C_n-Cr^{SNS}**, n = 0, 2, 6) non-negligible cooperative effects are observed in ethylene polymerization. Studies of **Ti-C_0-Cr^{SNS}**, **Ti-C_2-Cr^{SNS}** and **Ti-C_6-Cr^{SNS}** mediated ethylene polymerizations, carried out under identical conditions versus tandem mixtures of mononuclear Ti + Cr analogues, reveal marked conversion insensitive cooperative effects as indexed by product M_ns, *n*-butyl branch densities, and the conversion dependence thereof, which scale roughly inversely with accessible metal···metal distance. Specifically, with ethylene as the feed and MAO as cocatalyst/activator, SNS-based complexes **Ti-C_0-Cr^{SNS}**, **Ti-C_2-Cr^{SNS}**, and **Ti-C_6-Cr^{SNS}** afford LLDPEs with exclusive *n*-butyl branches (6.8−25.8 branches/1000 C). In addition, **Ti-C_0-Cr^{SNS}** produces polyethylenes with higher activity (4.5× and 6.1×, respectively), M_n (1.3× and 1.8×, respectively), and branch density (1.4× and 3.8×, respectively), than do **Ti-C_2-Cr^{SNS}** and **Ti-C_6-Cr^{SNS}**. With respect to the **CGC^{Et}Ti** + **SNSCr** tandem catalyst, **Ti-C_0-Cr^{SNS}** yields polyethylene with lower activity, but with 22.6× higher M_n, and 4.0× greater branch density under identical conditions. Furthermore, it is possible that 1-hexene binding partially blocks/competes for ethylene activation and enchainment sites, explaining the reduced polymerization activity compared to **CGC^{Et}Ti**. In addition, the present results show that metal proximity can modify the catalytic environment to increase the propagation/termination rate ratios, in turn favoring increased product M_n. Importantly, chain transfer to monomer is the predominant chain transfer pathway (Scheme 3, Path C)

Scheme 3. Plausible Pathway for 1-Hexene Generation and Subsequent Copolymerization with Ethylene Mediated by the Heterobimetallic Catalyst Ti-C_0-Cr^{SNS}

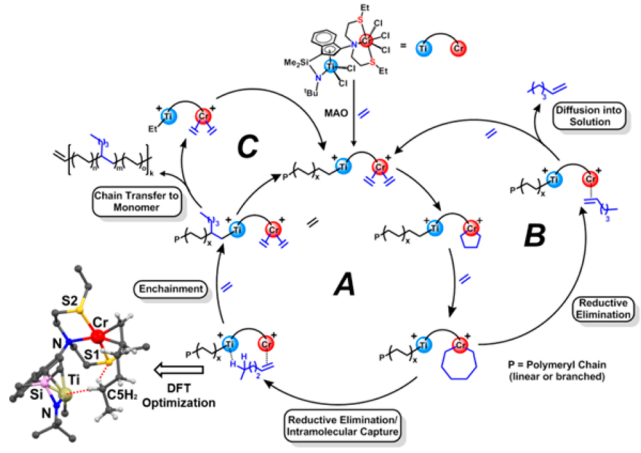

operative in these heterobimetallic catalysts, with an extraordinary >98% of vinylene end-group content in the case of **Ti-C_0-Cr^{SNS}**. Moreover, polymerization activity and comonomer enchainment selectivity are strongly influenced by cocatalyst/activator ($^iBu_3Al$/$[Ph_3C][B(C_6F_5)_4]$, $^iBu_3Al$/-$B(C_6F_5)_3$, or MMAO), polymerization solvent (toluene vs chlorobenzene), and ligand structure (**Ti-C_2-Cr^{PNP}** and **Ti-C_2-Cr^{NNN}**).

3.2. Catalytic Center Proximity Effects: Mechanism. The foregoing data and discussion strongly argue that covalently linking the dissimilar catalytic sites in **Ti-C_0-Cr^{SNS}**, **Ti-C_2-Cr^{SNS}**, and **Ti-C_6-Cr^{SNS}** spatially confines the catalytic centers in such a way that the efficiency and integrity of transfer of the 1-hexene comonomer produced at the Cr centers (established oligomer maker) to the Ti centers (established polymer maker) is significantly increased. This essentially intramolecular/concerted enchainment efficiency as well as exclusion of competing α-olefin is dramatically evident in **Ti-C_0-Cr^{SNS}** which has the shortest linkage and closest computed metal···metal proximity. A reasonable scenario for 1-hexene enchainment at Ti with cooperation of Cr is depicted in Scheme 3. It is likely that coordination of Cr-derived 1-hexene to the cationic Ti center is stabilized by the proximate Cr center and Ti-olefin agostic interactions as supported by the DFT calculations and that this cooperativity enhances the subsequent enchainment probability (Scheme 3, Path A). Moreover, the DFT modeling suggests that 1-hexene enchainment selection

dx.doi.org/10.1021/ja5046742 | J. Am. Chem. Soc. 2014, 136, 10460−10469

by **Ti-C_0-Cr^{SNS}** versus **Ti-C_2-Cr^{SNS}** is enhanced by substrate binding, which may include a C-H···S interaction (Figure 4). Also, as discussed above for the precatalysts, the metal−metal distances can fluctuate due to the conformational mobility about the bridging fragment, and, in turn, this mobility increases with the bridge length. Obviously, a rigid system in which the distance between the two metals is well-suited for promoting α-olefin π-bonding and agostic interactions should exhibit enhanced cooperativity with respect to more flexible systems in which the most selective conformation is not rigorously enforced. In this context, it would be expected that **Ti-C_0-Cr^{SNS}** would exhibit higher copolymerization performance than **Ti-C_2-Cr^{SNS}** and **Ti-C_6-Cr^{SNS}**. Note also that part of the 1-hexene produced at the Cr center escapes from the bimetallic coordination sphere and diffuses into the surrounding medium (Scheme 3, Path B). However, "free" 1-hexene is minimally incorporated into the polyethylene backbone, as confirmed the by 1-pentene competition experiments. Here, despite increased concentrations of available "free" α-olefin, the present heterobimetallic catalysts preferentially enchain *n*-butyl branches in densities which are high and essentially independent of conversion/increasing 1-hexene concentration. Treating the 1-hexene enchainment at **Ti-C_0-Cr^{SNS}** as an intramolecular process ($\nu_{intra} = k_{butyl\ branch}$[Ti]) and 1-pentene enchainment as an intermolecular process ($\nu_{inter} = k_{propyl\ branch}$[Ti][1-pentene]), assuming that [ethylene] remains constant and functions essentially the same in both enchainment reactions and that branch−branch interactions are not important, then the effective local concentration (M)[58] of 1-hexene can be found by estimating $k_{butyl\ branch}/k_{propyl\ branch}$. This is done by extrapolating the (linear) plot of butyl:propyl branch ratio versus [1-pentene] (Figure S38) to the point where the branch densities are equal and solving for $k_{butyl\ branch}/k_{propyl\ branch}$. For **Ti-$C_0$-$Cr^{SNS}$** M is found to be a rather large ∼8.6 M. While classical solvent cage effects[59] could in principle contribute to confining 1-hexene in the reaction zone, these cannot be rigorously ruled out, and experiments to probe for them (e.g., change of solvent viscosity) would be complicated by competing mass transfer effects, both micro- and macroscopic.

4. CONCLUSIONS

The present results significantly expand the scope of what is known about metal···metal proximity and cocatalyst/solvent effects in cooperative heterobimetallic olefin polymerization catalysis. In ethylene homopolymerization, both the product molecular M_ns and branch densities, in the order, **Ti-C_0-Cr^{SNS}** > **Ti-C_2-Cr^{SNS}** > **Ti-C_6-Cr^{SNS}** > **CGCTi** + **SNSCr**, roughly scale inversely with metal···metal distance under identical polymerization conditions with an MAO cocatalyst in toluene. In the ethylene + 0.10 M 1-pentene competition experiments, **Ti-C_0-Cr^{SNS}** incorporates *n*-propyl branches at 5.5% of the total branches, while the metrics for **Ti-C_2-Cr^{SNS}**, **Ti-C_6-Cr^{SNS}**, and tandem **CGCTi** + **SNSCr** are 34.8%, 55.1%, and 91.0%, respectively. When the polar C_6H_5Cl is used as the polymerization medium, thereby weakening the catalyst-cocatalyst ion pairing, substantial alterations in catalyst response and polymer product properties are observed. Homopolymerization, copolymerization, and DFT computational results argue that achievable Ti···Cr spatial proximity markedly influences chain transfer rates and selectivity for comonomer enchainment and that such proximity effects are relatively conversion insensitive but cocatalyst, solvent, and ligand framework sensitive.

■ ASSOCIATED CONTENT

Supporting Information

Details of ligand and catalyst synthesis/characterization, **CGCTiCl_2-C_0-SNS** crystallographic details (CIF), polymerization experiments, polymer characterization, and DFT calculations. This material is available free of charge via the Internet at http://pubs.acs.org.

■ AUTHOR INFORMATION

Corresponding Authors

m-delferro@northwestern.edu
t-marks@northwestern.edu

Notes

The authors declare no competing financial interest.

■ ACKNOWLEDGMENTS

Financial support by NSF (Grant CHE-1213235) and DOE (Grant 86ER13511) is gratefully acknowledged. Purchases of the NMR and GC−TOF instrumentation at the IMSERC at Northwestern U. were supported by NSF (Grant CHE-1048773 and CHE-0923236, respectively). High performance computational resources supporting this work were provided by the Northwestern Univ. Quest High Performance Computing (HPC) cluster and by CINECA (award HP10CBHAYD) under the ISCRA initiative. We also thank Albemarle Co. for the generous gifts of $B(C_6F_5)_3$, $[Ph_3C]^+[B(C_6F_5)_4]^-$, and MMAO.

■ REFERENCES

(1) (a) Haak, R. H.; Wezenberg, S. J.; Kleij, A. W. *Chem. Commun.* **2010**, *46*, 2713−2723. (b) Mitić, N.; Smith, S. J.; Neves, A.; Guddat, L. W.; Gahan, L. R.; Schenk, G. *Chem. Rev.* **2006**, *106*, 3338−3363.

(2) Jabri, E.; Carr, M. B.; Hausinger, R. P.; Karplus, P. A. *Science* **1995**, *268*, 998−1004.

(3) Sträter, N.; Lipscomb, W. N.; Klabunde, T.; Krebs, B. *Angew. Chem., Int. Ed. Engl.* **1996**, *35*, 2024−2055.

(4) Paull, D. H.; Abraham, C. J.; Scerba, M. T.; Alden-Danforth, E.; Lectka, T. *Acc. Chem. Res.* **2008**, *41*, 655−663.

(5) Belle, C.; Pierre, J. L. *Eur. J. Inorg. Chem.* **2003**, 4137−4146.

(6) (a) Matsunaga, S.; Shibasaki, M. *Chem. Commun.* **2014**, *50*, 1044−1057. (b) Hetterscheid, D. G. H.; Chikkali, S. H.; de Bruin, B.; Reek, J. N. H. *ChemCatChem.* **2013**, *5*, 2785−2793. (c) Bratko, I.; Gomez, M. *Dalton Trans.* **2013**, *42*, 10664−10681.

(7) Sone, T.; Yamaguchi, A.; Matsunaga, S.; Shibasaki, M. *J. Am. Chem. Soc.* **2008**, *130*, 10078−10079.

(8) (a) Delferro, M.; Marks, T. J. *Chem. Rev.* **2011**, *111*, 2450−2485. (b) Li, H.; Marks, T. J. *Proc. Natl. Acad. Sci. U.S.A.* **2006**, *103*, 15295−15302.

(9) (a) Gibson, V. C.; Spitzmesser, S. K. *Chem. Rev.* **2003**, *103*, 283−316. (b) Ittel, S. D.; Johnson, L. K.; Brookhart, M. *Chem. Rev.* **2000**, *100*, 1169−1204.

(10) (a) Braunschweig, H.; Breitling, F. M. *Coord. Chem. Rev.* **2006**, *250*, 2691−2720. (b) McKnight, A. L.; Waymouth, R. M. *Chem. Rev.* **1998**, *98*, 2587−2598.

(11) (a) Motta, A.; Fragala, I. L.; Marks, T. J. *J. Am. Chem. Soc.* **2009**, *131*, 3974−3984. (b) Guo, N.; Stern, C. L.; Marks, T. J. *J. Am. Chem. Soc.* **2008**, *130*, 2246−2261. (c) Li, H.; Li, L.; Schwartz, D. J.; Metz, M. V.; Marks, T. J.; Liable-Sands, L.; Rheingold, A. L. *J. Am. Chem. Soc.* **2005**, *127*, 14756−14768. (d) Li, H.; Li, L.; Marks, T. J. *Angew. Chem., Int. Ed.* **2004**, *43*, 4937−4940.

(12) (a) Salata, M. R.; Marks, T. J. *Macromolecules* **2009**, *42*, 1920−1933. (b) Salata, M. R.; Marks, T. J. *J. Am. Chem. Soc.* **2008**, *130*, 12−13.

(13) (a) Weberski, M. P.; Chen, C. L.; Delferro, M.; Marks, T. J. *Chem.—Eur. J.* **2012**, *18*, 10715−10732. (b) Rodriguez, B. A.; Delferro, M.; Marks, T. J. *Organometallics* **2008**, *27*, 2166−2168.

(14) Makio, H.; Terao, H.; Iwashita, A.; Fujita, T. *Chem. Rev.* **2011**, *111*, 2363−2449.
(15) Li, L.; Metz, M. V.; Li, H.; Chen, M.-C.; Marks, T. J.; Liable-Sands, L.; Rheingold, A. L. *J. Am. Chem. Soc.* **2002**, *124*, 12725−12741.
(16) (a) Robert, C.; Thomas, C. M. *Chem. Soc. Rev.* **2013**, *42*, 9392−9402. (b) McGuinness, D. S. *Chem. Rev.* **2011**, *111*, 2321−2341. (c) Komon, Z. J. A.; Bazan, G. C. *Macromol. Rapid Commun.* **2001**, *22*, 467−478.
(17) (a) Schwerdtfeger, E. D.; Price, C. J.; Chai, J. F.; Miller, S. A. *Macromolecules* **2010**, *43*, 4838−4842. (b) de Wet-Roos, D.; Dixon, J. T. *Macromolecules* **2004**, *37*, 9314−9320.
(18) Wang, J.; Li, H.; Guo, N.; Li, L.; Stern, C. L.; Marks, T. J. *Organometallics* **2004**, *23*, 5112−5114.
(19) Liu, S.; Motta, A.; Delferro, M.; Marks, T. J. *J. Am. Chem. Soc.* **2013**, *135*, 8830−8833.
(20) (a) Agapie, T. *Coord. Chem. Rev.* **2011**, *255*, 861−880. (b) Wass, D. F. *Dalton Trans.* **2007**, 816−819.
(21) McGuinness, D. S.; Wasserscheid, P.; Keim, W.; Morgan, D.; Dixon, J. T.; Bollmann, A.; Maumela, H.; Hess, F.; Englert, U. *J. Am. Chem. Soc.* **2003**, *125*, 5272−5273.
(22) Motta, A.; Fragala, I. L.; Marks, T. J. *J. Chem. Theory Comput.* **2013**, *9*, 3491−3497.
(23) Bochmann, M. *Organometallics* **2010**, *29*, 4711−4740.
(24) (a) Yang, Y.; Liu, Z.; Zhong, L.; Qiu, P. Y.; Dong, Q.; Cheng, R. H.; Vanderbilt, J.; Liu, B. P. *Organometallics* **2011**, *30*, 5297−5302. (b) Agapie, T.; Labinger, J. A.; Bercaw, J. E. *J. Am. Chem. Soc.* **2007**, *129*, 14281−14295.
(25) Agapie, T.; Schofer, S. J.; Labinger, J. A.; Bercaw, J. E. *J. Am. Chem. Soc.* **2004**, *126*, 1304−1305.
(26) Liu, S.; Pattacini, R.; Braunstein, P. *Organometallics* **2011**, *30*, 3549−3558.
(27) (a) Stephenson, C. J.; McInnis, J. P.; Chen, C.; Weberski, M. P.; Motta, A.; Delferro, M.; Marks, T. J. *ACS Catal.* **2014**, *4*, 999−1003. (b) Weberski, M. P.; Chen, C. L.; Delferro, M.; Zuccaccia, C.; Macchioni, A.; Marks, T. J. *Organometallics* **2012**, *31*, 3773−3789.
(28) Severn, J. R.; Chadwick, J. C.; Duchateau, R.; Friederichs, N. *Chem. Rev.* **2005**, *105*, 4073−4147.
(29) Bochmann, M. *Acc. Chem. Res.* **2010**, *43*, 1267−1278.
(30) (a) Seger, M. R.; Maciel, G. E. *Anal. Chem.* **2004**, *76*, 5734−5747. (b) Galland, G. B.; de Souza, R. F.; Mauler, R. S.; Nunes, F. F. *Macromolecules* **1999**, *32*, 1620−1625.
(31) Bowen, L. E.; Charernsuk, M.; Hey, T. W.; McMullin, C. L.; Orpen, A. G.; Wass, D. F. *Dalton Trans.* **2010**, *39*, 560−567.
(32) Möhring, P. C.; Coville, N. J. *Coord. Chem. Rev.* **2006**, *250*, 18−35.
(33) Klosin, J.; Kruper, W. J.; Nickias, P. N.; Roof, G. R.; De Waele, P.; Abboud, K. A. *Organometallics* **2001**, *20*, 2663−2665.
(34) Jabri, A.; Temple, C.; Crewdson, P.; Gambarotta, S.; Korobkov, I.; Duchateau, R. *J. Am. Chem. Soc.* **2006**, *128*, 9238−9247.
(35) Green, M. L. H.; Popham, N. H. *J. Chem. Soc., Dalton Trans.* **1999**, 1049−1059.
(36) Li, H.; Stern, C. L.; Marks, T. J. *Macromolecules* **2005**, *38*, 9015−9027.
(37) Liu, Z.; Somsook, E.; White, C. B.; Rosaaen, K. A.; Landis, C. R. *J. Am. Chem. Soc.* **2001**, *123*, 11193−11207.
(38) Chen, E. Y.-X.; Marks, T. J. *Chem. Rev.* **2000**, *100*, 1391−1434.
(39) Guan, Z.; Cotts, P. M.; McCord, E. F.; McLain, S. J. *Science* **1999**, *283*, 2059−2062.
(40) (a) Roberts, J. A. S.; Chen, M.-C.; Seyam, A. M.; Li, L.; Zuccaccia, C.; Stahl, N. G.; Marks, T. J. *J. Am. Chem. Soc.* **2007**, *129*, 12713−12733. (b) Chen, M. C.; Roberts, J. A. S.; Seyam, A. M.; Li, L. T.; Zuccaccia, C.; Stahl, N. G.; Marks, T. J. *Organometallics* **2006**, *25*, 2833−2850.
(41) Wang, J. F.; Wang, L.; Gao, H. Q.; Wang, W. Q.; Jiang, G. H.; Dong, X. H.; Wang, W.; Feng, L. F. *Polym. Eng. Sci.* **2007**, *47*, 540−544.
(42) (a) Walter, M. D.; White, P. S.; Brookhart, M. *Chem. Commun.* **2009**, 6361−6363. (b) Chirik, P. J.; Bercaw, J. E. *Organometallics* **2005**, *24*, 5407−5423.
(43) Zheng, P.; Takayama, S.-i. J.; Mauk, A. G.; Li, H. *J. Am. Chem. Soc.* **2012**, *134*, 4124−4131.
(44) (a) Baba, K.; Okamura, T.-a.; Yamamoto, H.; Yamamoto, T.; Ohama, M.; Ueyama, N. *Inorg. Chem.* **2006**, *45*, 8365−8371. (b) Ma, C. L.; Zhang, Q. F.; Zhang, R. F.; Wang, D. Q. *Chem.—Eur. J.* **2006**, *12*, 420−428. (c) Lin, I.-J.; Gebel, E. B. *Proc. Natl. Acad. Sci. U. S. A.* **2005**, *102*, 14581−14586.
(45) Braunstein, P.; Naud, F. *Angew. Chem., Int. Ed.* **2001**, *40*, 680−699.
(46) Nomura, K.; Fudo, A. *Catal. Commun.* **2003**, *4*, 269−274.
(47) (a) McGuinness, D. S.; Rucklidge, A. J.; Tooze, R. P.; Slawin, A. M. Z. *Organometallics* **2007**, *26*, 2561−2569. (b) McGuinness, D. S.; Brown, D. B.; Tooze, R. P.; Hess, F. M.; Dixon, J. T.; Slawin, A. M. Z. *Organometallics* **2006**, *25*, 3605−3610.
(48) McGuinness, D. S.; Wasserscheid, P.; Morgan, D. H.; Dixon, J. T. *Organometallics* **2005**, *24*, 552−556.
(49) Thapa, I.; Gambarotta, S.; Korobkov, I.; Duchateau, R.; Kulangara, S. V.; Chevalier, R. *Organometallics* **2010**, *29*, 4080−4089.
(50) Licciulli, S.; Thapa, I.; Albahily, K.; Korobkov, I.; Gambarotta, S.; Duchateau, R.; Chevalier, R.; Schuhen, K. *Angew. Chem., Int. Ed.* **2010**, *49*, 9225−9228.
(51) Smiles, D. E.; Wu, G.; Hayton, T. W. *J. Am. Chem. Soc.* **2014**, *136*, 96−99.
(52) McGuinness, D. S.; Overett, M.; Tooze, R. P.; Blann, K.; Dixon, J. T.; Slawin, A. M. Z. *Organometallics* **2007**, *26*, 1108−1111.
(53) Atiqullah, M.; Hammawa, H.; Hamid, H. *Eur. Polym. J.* **1998**, *34*, 1511−1520.
(54) Bouwkamp, M. W.; de Wolf, J.; del Hierro Morales, I.; Gercama, J.; Meetsma, A.; Troyanov, S. I.; Hessen, B.; Teuben, J. H. *J. Am. Chem. Soc.* **2002**, *124*, 12956−12957.
(55) Kawabe, M.; Murata, M. *Macromol. Chem. Phys.* **2001**, *202*, 2440−2446.
(56) Carter, A.; Cohen, S. A.; Cooley, N. A.; Murphy, A.; Scutt, J.; Wass, D. F. *Chem. Commun.* **2002**, 858−859.
(57) Junges, F.; Kuhn, M. C. A.; Dos Santos, A. H. D. P.; Rabello, C. R. K.; Thomas, C. M.; Carpentier, J.-F.; Casagrande, O. L., Jr. *Organometallics* **2007**, *26*, 4010−4014.
(58) Raynal, M.; Ballester, P.; Vidal-Ferran, A.; van Leeuwen, P. W. N. M. *Chem. Soc. Rev.* **2014**, *43*, 1660−1733.
(59) Koenig, T. W.; Hay, B. P.; Finke, R. G. *Polyhedron* **1988**, *7*, 1499−516.